

## Foundations of chemical microscopy.

# 1. Solid-state characterization of 5-nitrobarbituric acid (dilituric acid) and its complexes with Group IA and Group IIA cations

Harry G. Brittain \*

*Ohmeda Pharmaceutical Products Division, BOC Group Technical Center, 100 Mountain Avenue, Murray Hill, NJ 07974, USA*

Received 27 June 1996; accepted 6 August 1996

### Abstract

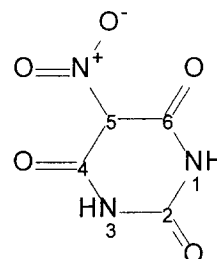
5-Nitrobarbituric acid (dilituric acid) has been used as a chemical microscopic reagent for the qualitative identification of alkali metal (Group IA) and alkaline earth (Group IIA) cations. This methodology was based on the characterization of observed crystal morphologies, since a unique crystal habit could be associated with each adduct product. To understand the scientific foundations which permitted chemical microscopy to function as a useful analytical technique, the products formed between dilituric acid and the Group IA and IIA cations were characterized using polarizing optical microscopy, powder X-ray diffraction, thermal analysis and solid-state nuclear magnetic resonance. It was found that the origins of the different crystal morphologies associated with each of the adduct arose from the ability of the systems to form various hydrate species, which could also contain structural variations due to cation/diliturate packing patterns. © 1997 Elsevier Science B.V.

**Keywords:** Microscopy; 5-Nitrobarbituric acid; Dilituric acid; Group IA cations; Group IIA cations

### 1. Introduction

One of the most important analytical techniques used during the first half of this century was chemical microscopy. For this approach of analysis, derivatives of the analyte species were prepared, crystallized and identified by means of the morphological characteristics of the resulting adducts [1]. For example, Dunbar and his associates used a series of reagents to develop specific tests for amines [2,3], carboxylic acids, anhydrides and acid chlorides [4,5], aldehydes and ketones

[6], hydroxy compounds [7], amino acids [8] and cations [9]. In another extensive series of studies, Clarke and coworkers developed sensitive microchemical tests for the determination of alkaloids [10,12,16], anesthetics [11], antihistamines [13], antimalarials [14] and analgesics [15].



\* Tel.: +1 201 7637214; fax: +1 201 7630980. Present address: Acute Therapeutics, Inc., 88 Courter Avenue, Maplewood, NJ 07040, USA.

During the course of this type of work, it was found that 5-nitrobarbituric acid (dilituric acid), was the reagent of choice for the identification of primary and secondary amines because of its easy preparation and purification, its moderate solubility, and its acidic nature and consequent ability to react with basic compounds [17]. Most important, however, was the high degree of crystallinity and ease of recrystallization associated with its adduct compounds. It was also noted at this time that the solubility of the potassium salt and the solubilities of the salts of divalent alkaline earth cations, were extremely low. This finding was exploited by Francis, who developed chemical microscopic identification techniques for cations which were based solely on the morphology of isolated precipitates [18].

Workers skilled in the art could therefore readily use precipitation with dilituric acid as a means to identify the alkali metal (Group IA) or alkaline earth (Group IIA) cations entirely on the basis of observed crystal morphologies. One of the more intriguing aspects of these investigations and the never-asked question, was why should each and every adduct exhibit a unique crystal morphology in the first place?

To more fully understand the scientific foundations which permitted chemical microscopy to function as a useful analytical technique, a detailed structural investigation into the solid state behavior of dilituric acid and its insoluble cation salts was conducted. Materials were characterized using polarizing optical microscopy, powder X-ray diffraction, thermal analysis and solid-state nuclear magnetic resonance, with the ultimate aim of deducing the underlying principles governing the production of characteristic crystal morphologies.

## 2. Experimental

### 2.1. Chemicals

Dilituric acid was obtained from the Aldrich Chemical Company (Milwaukee, WI) in the highest purity available and was used without subsequent purification. Alkali metal or alkaline

earth chlorides or nitrates were used as the source of cations, and were obtained as reagent grade materials from Aldrich.

### 2.2. Preparation of cation adducts

The diliturate adducts were prepared by suspending 1 mmol of dilituric acid and 1 mmol of metal cation in 5–10 ml of deionized water, shaking vigorously for 1 min, and then heating at 60°C until the contents were completely dissolved. Upon cooling to room temperature, the derivatives precipitated as crystalline products which were allowed to air-dry prior to their analysis. Each adduct was prepared in duplicate and the optical microscopic characteristics of each lot compared. In every instance, identical adduct products were produced.

### 2.3. Equipment

#### 2.3.1. Polarizing optical microscopy

Optical microscopic investigations were conducted on a Nikon Labophot-2 compound microscope system, at magnifications between 40× and 200× (depending on the particle size). Samples were immersed in mineral oil, and held on the slide under a cover glass. The samples were viewed using ordinary illumination, and between crossed polarizers to evaluate the degree of crystallinity. Hot-stage microscopic characterizations were carried out using a simple Kofler device.

#### 2.3.2. Thermal analysis

Measurements of thermogravimetry were obtained on a Perkin-Elmer TGA-7 thermal analysis system. Approximately 5 mg of sample was placed on the pan, and inserted in the TG furnace. The sample was then heated at a rate of 10°C min<sup>-1</sup>, up to a final temperature of 250°C.

#### 2.3.3. Powder X-ray diffraction

The X-ray powder patterns of the samples were obtained using a Philips model APD 3720 powder diffraction system, equipped with a vertical goniometer configured in the  $\theta/2\text{-}\theta$  geometry. The K- $\alpha$  line of copper (1.544056 Å) was used as the



Fig. 1. Morphology of recrystallized dilituric acid, obtained using optical microscopy at a magnification of  $200\times$ .

radiation source. Each sample was scanned between  $2$  and  $40^\circ$   $2-\theta$ , at a scan rate of  $0.02$  degrees  $2-\theta$   $s^{-1}$ .

#### 2.3.4. Solid-state nuclear magnetic resonance

Solid-state  $^{13}\text{C}$ -NMR spectra were acquired at Spectral Data Services, (Champaign, IL) at a field strength of  $270$  MHz. All spectra were obtained using the cross polarization, magic angle spinning (CP/MAS) pulse sequence.

### 3. Results and discussion

#### 3.1. Dilituric acid trihydrate

The solid-state characteristics of the dilituric acid reagent were first evaluated to assemble a background of appropriate data to be used during the interpretation of analogous data obtained on the derivative species. Dilituric acid was accordingly recrystallized according to the protocol used for generation of the adduct precipitates and subjected to the full range of characterization. As shown in Fig. 1, the compound was obtained as

tabular plates, which were found to exhibit only first-order birefringence owing to their thinness.

The water content of recrystallized dilituric acid was obtained using thermogravimetry. The TG thermogram consisted of a  $23.8\%$  weight loss by  $150^\circ\text{C}$  and a further loss of approximately  $17\%$  by  $190^\circ\text{C}$ . The first weight loss is assigned to the loss of lattice water, and correlates well with the theoretical weight loss of  $23.9\%$  anticipated for an authentic trihydrate phase. The second weight loss is certainly associated with the exothermic decomposition of the compound. The thermogravimetry observations were confirmed using hot-stage microscopy, where the evolution of decomposition products over these temperature ranges was observed for solid immersed in mineral oil and observed visually during the heating process.

The single-crystal structure of dilituric acid trihydrate has been reported in the literature [19]. In the reported structure, the dilituric acid molecules form hydrogen-bonded sheets which are essentially coplanar, and parallel to the  $(010)$  plane. The water molecules are hydrogen-bonded in the channels formed by the 3-dimensional placement of the sheet planes. The recrystallized dilituric

acid formed in the present study was obtained as a highly crystalline product, as evident by its well-defined X-ray powder diffraction pattern (Fig. 2).

As illustrated in Fig. 3, the solid-state  $^{13}\text{C}$ -NMR spectrum of dilituric acid consisted of three resonances observed at 112.7, 152.4 and 163.1 ppm. Since there are only four carbon atoms in the molecule (all contained in the ring structure), assignment of the observed resonances is not difficult. Following the numbering system shown earlier, the resonance at 112.7 ppm is assigned to carbon-5, the carbon at which the nitro group is bound. The resonance at 152.4 ppm is assigned to carbon-2 and the resonance at 163.1 ppm is assigned to the magnetically equivalent nuclei at carbon-4 and carbon-6. These assignments are based on the conclusions deduced from solution-phase studies, where it was concluded that carbon-5 resonated at 112.9 ppm, carbon-2 at 149.9 ppm, and the magnetically equivalent carbons-4/6 at 159.6 ppm [20].

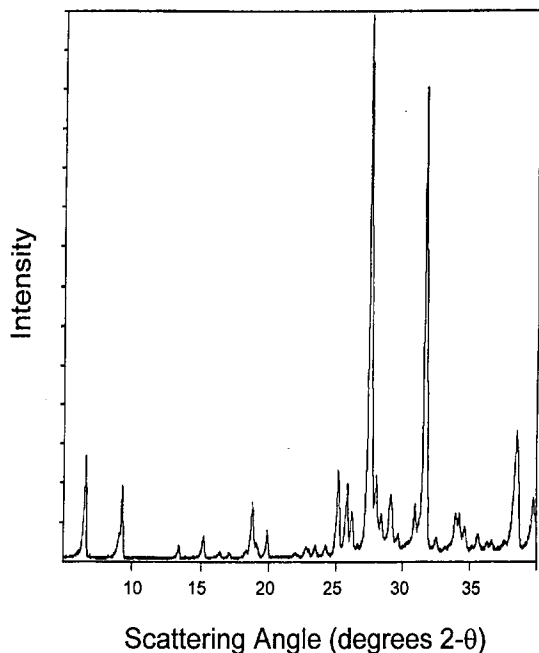


Fig. 2. Powder X-ray diffraction pattern of recrystallized dilituric acid.

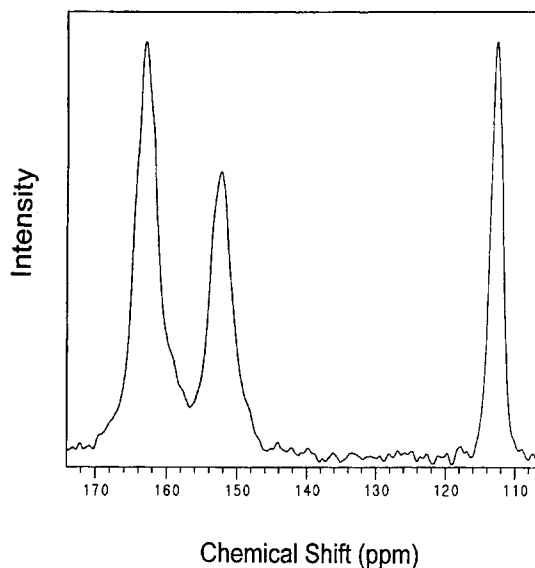


Fig. 3. Solid-state  $^{13}\text{C}$ -NMR spectrum of recrystallized dilituric acid.

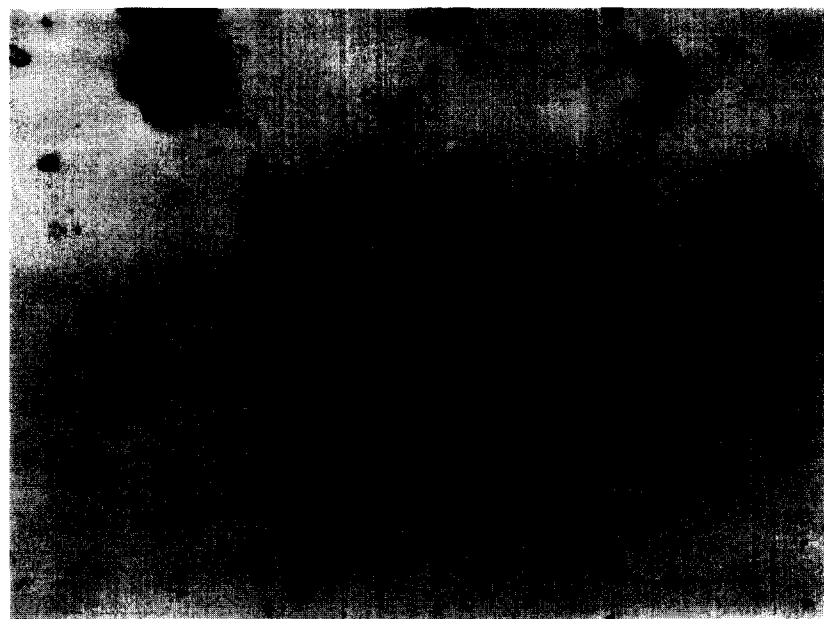
### 3.2. Adducts formed with Group IA cations

As noted in previous work [18], the crystalline products formed between dilituric acid and Group IA cations each differed from each other with respect to their morphological properties. These differences are illustrated in Fig. 4, where it may also be noted that the morphologies of the adducts are readily distinguishable from that of the dilituric acid reagent as well. The Li-DLA adduct was observed to form as irregular equant particles, the Na-DLA adduct as flat triangular prisms, the K-DLA and Rb-DLA adducts as tabular crystals and the Cs-DLA adduct as elongated tabular crystals. The relatively thin nature of the isolated adducts was evident in the low degree of birefringence obtained for each species, which was generally of first-order.

Thermogravimetric analysis was used to obtain the water content of the diliturate derivatives and to deduce the solvation state within the isolated adducts. This information is summarized in Table 1. With the exception of the Li-DLA adduct (which was obtained as a dihydrate species), the products formed between dilituric acid and the Group IA cations were all anhydrous. Unlike the

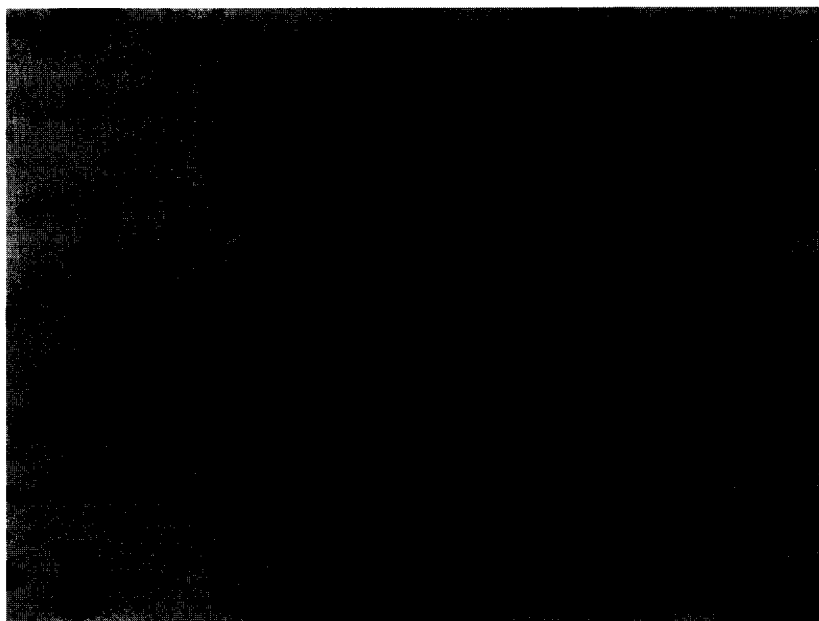


(a)



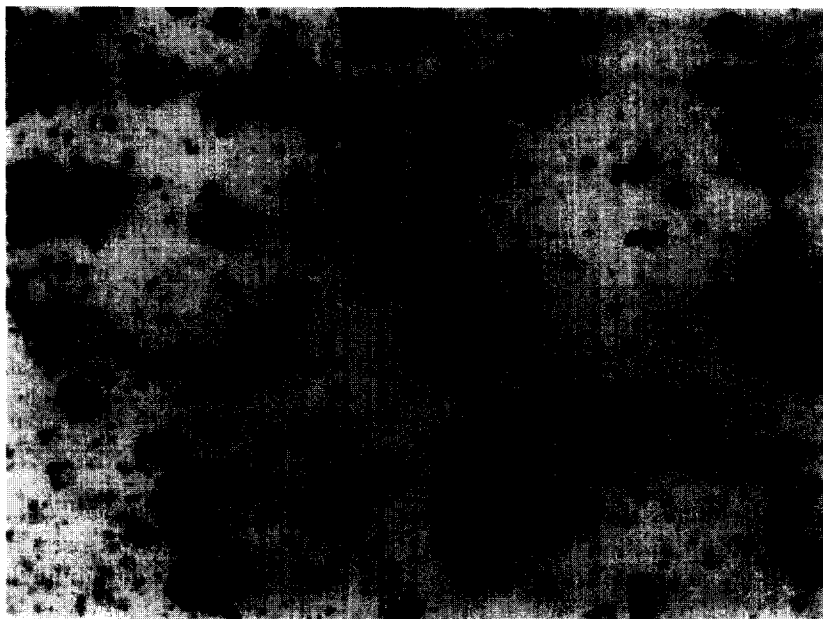
(c)

Fig. 4. Morphology of the products formed between diluturic acid and Group IA cations. Optical photomicrographs (obtained at a magnification of  $200\times$ ) are shown for (a) Li-DLA, (b) Na-DLA, (c) K-DLA, (d) Rb-DLA and (e) Cs-DLA.



(d)

Fig. 4.



(e)

Fig. 4.

dilituric acid reagent, the Na-DLA, K-DLA, Rb-DLA and Cs-DLA products did not exhibit a secondary decomposition when heated to 190°C. The Li-DLA adduct lost only 6.8% between 150 and 190°C, which is significantly less than that of the dilituric acid reagent itself.

Even though four of the five adducts of Group IA cations with dilituric acid were anhydrous in nature, their crystal structures were all found to be different from each other. As evident in Fig. 5, the X-ray powder patterns of all adducts were found to be mutually non-equivalent, and also not equivalent to that of the dilituric acid reagent. Since most of the adducts were obtained in the same state of hydration, it must be concluded that the different cations lead to the existence of different packing patterns within the various crystal lattices. Assuming that the crystal structure is based on the networking of diliturate species, and that these sheets are linked by the included

cations, it follows that the driving force for producing the differing packing patterns would be associated with the varying ionic radii of the cations. The significant decrease in the diliturate/cation radius ratio which takes place as one transverse from lithium down to cesium manifests itself in the various crystal structures, and the different crystal structures in turn lead to the existence of different crystal morphologies.

The solid-state  $^{13}\text{C}$ -NMR spectra of the Group IA adducts each consisted of three resonances, and the measured spectra strongly resembled that obtained for the dilituric acid reagent. A summary of the NMR data is provided in Table 2, where it may be seen that the resonance positions noted for carbon-2 and the magnetically equivalent nuclei at carbon-4 and carbon-6 are barely different from the analogous resonances detected for the dilituric acid reagent. A small, but significant, downfield shift of the resonance associated with

Table 1  
Thermogravimetric analysis of the adducts of dilituric acid with Group IA and IIA cations

Cation	Volatile content, RT-150°C (%)	Theoretical volatile content for the <i>n</i> -hydrate species	Hydration state ( <i>n</i> )	Volatile content, 150-190°C (%)
Free acid	23.8	23.9	3	17.1
Lithium	12.3	12.2	2	6.8
Sodium	0	0	0	0
Potassium	0	0	0	0
Rubidium	0	0	0	0
Cesium	0	0	0	0
Beryllium	22.9	23.0	3	0
Magnesium	12.1	12.1	1.5	11.5
Calcium	3.9	4.1	0.5	6.3
Strontium	0	0	0	13.2
Barium	2.5	2.8	0.50	0

carbon-5 (the carbon containing the nitro group) was consistently observed for each of the adduct species. Since the tendency of Group IA cations is to interact exclusively with oxygen donor atoms whenever possible, the NMR findings indicates

that the bonding between the diliturate moiety and the metal cation is predominantly with the oxygens of the nitro group at the 5-position, and not with the ketone oxygens of the barbiturate ring.

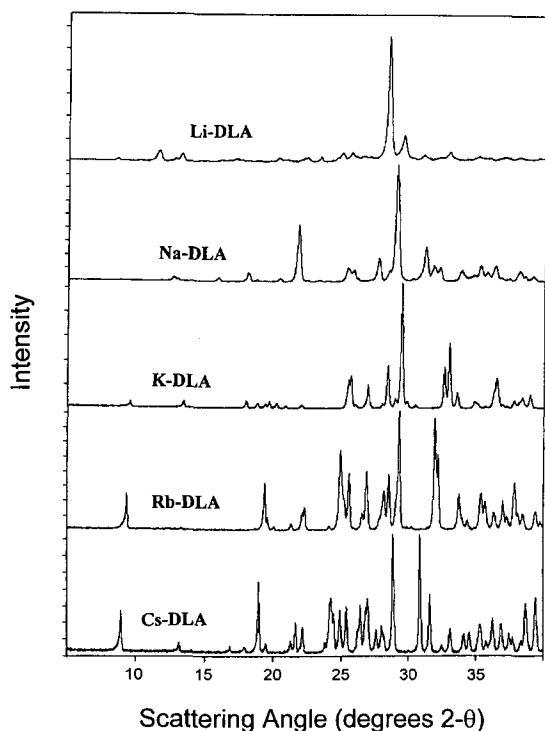


Fig. 5. Powder X-ray diffraction patterns of the Li-DLA, Na-DLA, K-DLA, Rb-DLA and Cs-DLA adduct products.

### 3.3. Adducts formed with Group IIA cations

It was found that not only did the crystalline products formed by dilituric acid with the Group IIA cations differ from each other in their morphological properties, they also differed in morphology relative to the adducts of the Group IA cations and from that of the dilituric acid reagent as well. Examples of the crystal morphologies obtained for the Group IIA cation adducts are illustrated in Fig. 6. The Be-DLA product was observed to form as flat rods, the ends of which were frequently found to be capped. On the other hand, the Mg-DLA product could only be obtained as a microcrystalline powder of indeterminate morphology. The Ca-DLA adduct precipitated in the form of long thin rods, while the Sr-DLA product consisted of small bundles of needle-like crystals. Finally, the Ba-DLA product formed as thick, almost equant rod-like crystals. Most crystals exhibited only first-order birefringence, although a significant number of the Ba-DLA crystals were sufficiently thick so as to enable the observation of higher-order birefringence colors.



Table 2  
Solid-state  $^{13}\text{C}$ -nuclear magnetic resonance bands obtained for the adducts of dilituric acid with Group IA and IIA cations

Cation	Chemical shift, Carbon-5 (ppm)	Chemical shift, Carbon-2 (ppm)	Chemical shift, Carbons-4,6 (ppm)
Free acid	112.7	152.4	163.1
Lithium	113.9	152.2	162.5
Sodium	113.8	152.6	162.6
Potassium	113.6	152.8	162.5
Rubidium	113.7	152.7	162.2
Cesium	113.5	152.3	162.5
Beryllium	113.3	151.9	162.8
Magnesium	112.5	151.6	163.1
Calcium	114.2	151.9	162.6
Strontium	112.8/116.0	152.6	160.4/164.4
Barium	116.2	151.9	160.1

The water content (and hence the solvation state) of the Group IIA cation diliturate adducts was established using thermogravimetric analysis, and this information has been included in Table 1. The variety of hydrate formation associated with the Group IIA cation adducts was found to be more extensive than was noted for the Group IA cation products. The Be-DLA product formed as a trihydrate species, the Mg-DLA product was obtained as a 1.5-hydrate and the Ca-DLA and Ba-DLA adducts were obtained as 0.5-hydrate species. The Sr-DLA product was obtained as an anhydrate phase.

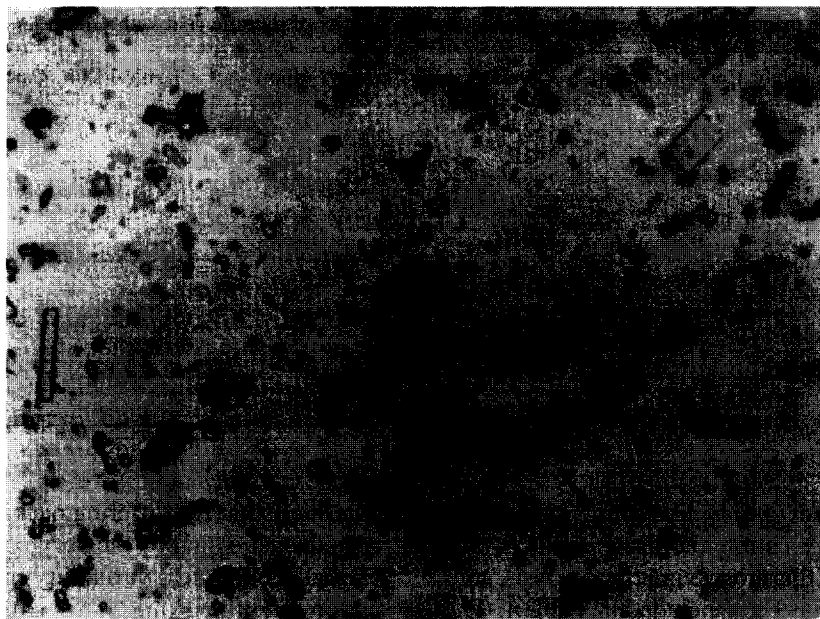
Unlike the dilituric acid reagent, the Be-DLA and Ba-DLA failed to exhibit a secondary decomposition when the sample heating was continued to 190°C. This behavior may be contrasted with that noted for the other Group IIA cation adduct species, where the Mg-DLA compound lost 11.5% between 150 and 190°C, the Ca-DLA adduct lost 6.3% and the Sr-DLA derivative lost only 13.2%. The lack of a secondary decomposition within the temperature range studied is taken as indicating an enhancement in crystal lattice energy relative to that of the dilituric acid reagent.

Given the variation in hydration state observed for the Group IIA cation adducts with dilituric acid, it is not surprising that each product yielded a unique crystal structure. This behavior is illustrated in Fig. 7, where it is evident that the X-ray powder patterns of all derivatives are mutually non-equivalent and not equivalent to dilituric acid.

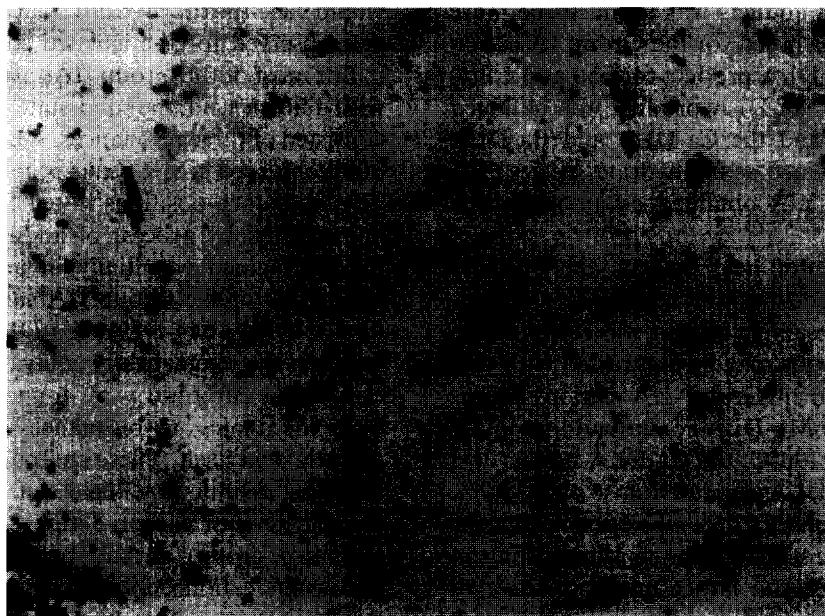
It is likely that the differing packing patterns which would exist owing to the varying ionic radii of the cations would yield variability in the nature of the cation/anion packing. This situation would certainly yield a variety of crystal structures, which would yield the range of different crystal morphologies observed for the isolated solids.

For most of the Group IIA cation adduct species with dilituric acid, the solid-state  $^{13}\text{C}$ -NMR spectra consisted of three resonances. A complete summary of all observed NMR peaks is collected in Table 2. The resonance positions noted for carbon-2 were not affected by process of adduct formation and these remained essentially invariant around 152 ppm in all of the Group IIA cation adducts. For the Be-DLA, Mg-DLA, Ca-DLA and Ba-DLA adducts, the magnetically equivalent nuclei at carbon-4 and carbon-6 were found to barely differ from the analogous resonances measured for the dilituric acid itself. These compounds all exhibited the same definite downfield shift of the resonance associated with carbon-5 (the carbon containing the nitro group) as had been observed for the Group IA cation derivative species. These NMR results indicates that the bonding between the diliturate moiety and the Group IIA metal cations is with the oxygens of the nitro group at the 5-position, and not with the ketone oxygens of the barbiturate ring.

The solid-state  $^{13}\text{C}$ -NMR spectrum of the Sr-DLA adduct was found to be anomalous in that the resonance bands associated with carbon-5



(a)

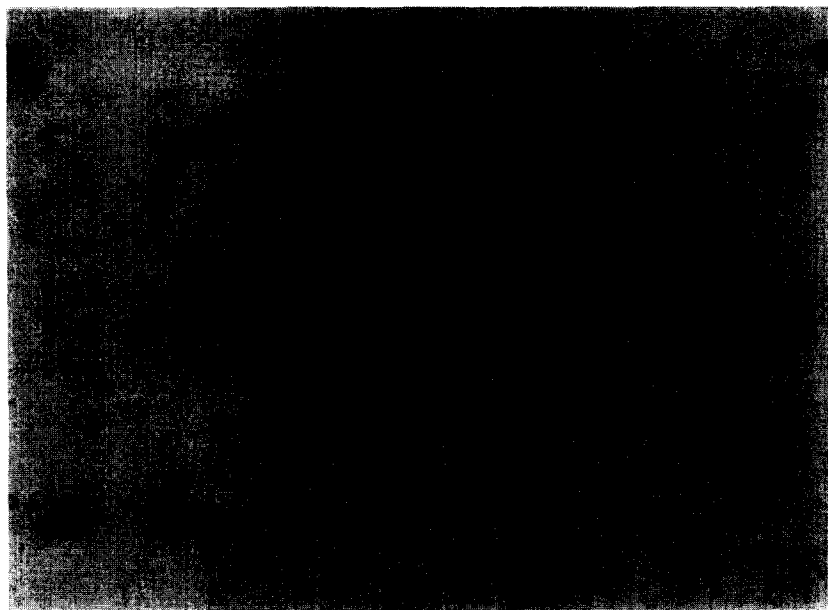


(b)

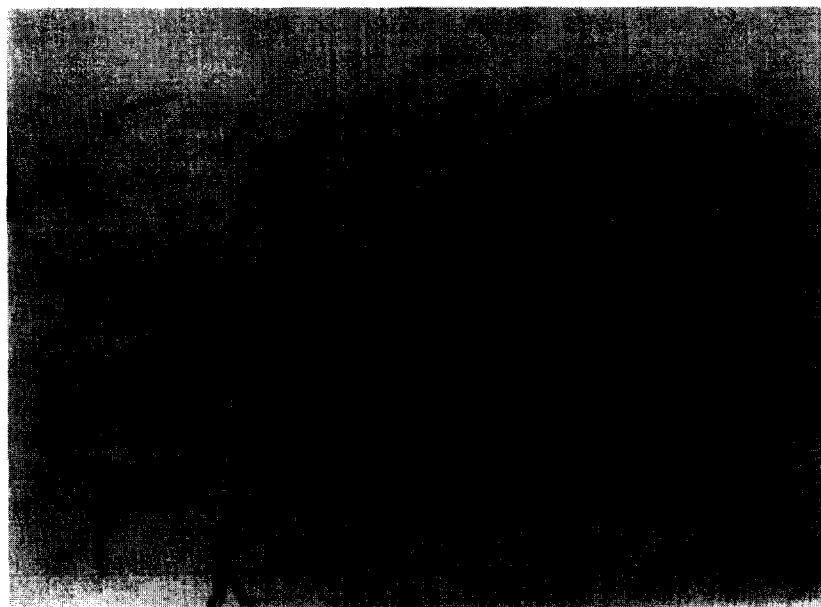
Fig. 6. Morphology of the products formed between dilituric acid and Group IIA cations. Optical photomicrographs (obtained at a magnification of  $200\times$ ) are shown for (a) Be-DLA, (b) Mg-DLA, (c) Ca-DLA, (d) Sr-DLA and (e) Ba-DLA.

and carbons-4/6 were split into two resonance bands. This observation would suggest that the Sr-DLA adduct crystallizes with two molecules in the unit cell, and that only carbon-2 is mag-

netically equivalent for each. Given the splitting in resonance bands derived from the carbon atoms containing the carbonyls adjacent to the 5-nitro group, it is possible that the solid



(c)



(d)

Fig. 6.

contains a mixed bonding combination. Within this view, half of the adduct species would form with the metal cation binding simply to the oxygens of the 5-nitro group. The other half of the adduct

species would exist as a result of chelate formation, where the metal cations would bridge between the oxygens of the 5-nitro group and with the adjacent ketone oxygen of the barbiturate ring.



(e)

Fig. 6.

The solid-state  $^{13}\text{C}$ -NMR spectrum of the Ba-DLA adduct was found to consist of a three band pattern, but the carbon-5 and carbon-4/6 peaks were observed at the resonance bands indicative of the postulated chelation. The spectral trends observed for the Ca-DLA, Sr-DLA, and Ba-DLA adduct species are illustrated in Fig. 8, which illustrates the shift in NMR resonances which takes place on passing from the middle to the bottom of Group IIA.

#### 4. Conclusions

The variety of morphologies observed for the Group IA and IIA cation adducts with 5-nitrobarbituric acid (dilituric acid) have been found to arise from the ability of this system to form numerous hydrates upon crystallization of the isolated solids. As demonstrated by the non-equivalence of X-ray powder patterns, each of the hydrate species exhibits a unique crystal structure. None of the crystalline adducts were found to be isomorphous, and this property is manifested in

differing crystal morphologies. When solids of equivalent hydration are obtained from solution, the differing cation/diliturate radius ratio values result in differing packing arrangements in the solids. These packing arrangements yield the variety of observed crystal structures and this polymorphism becomes evident in new crystal morphologies.

The ability of the 5-nitrobarbituric acid system to yield crystal morphologies which are diagnostic for the identification of Group IA and IIA cations can therefore be understood through the ability of the systems to form various hydrate species, which also contain structural variations due to cation/diliturate packing patterns.

#### Acknowledgements

Special appreciation is due to Patricia Rafalko for carrying out the powder X-ray diffraction and to Sarah Verbeeke for the thermal analysis work.

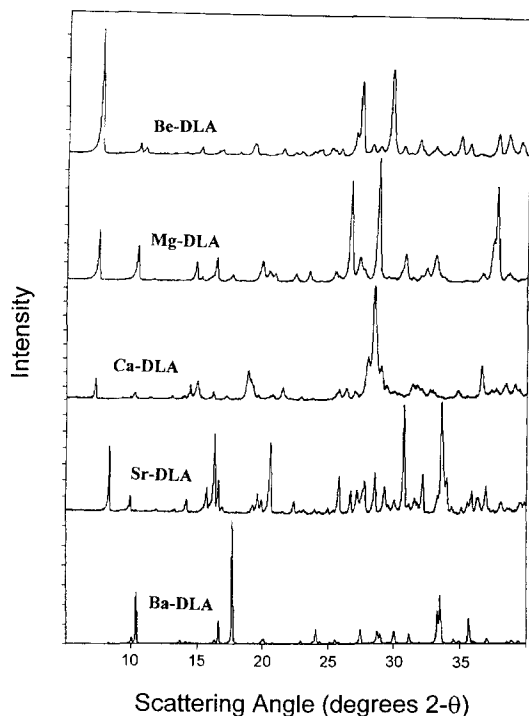


Fig. 7. Powder X-ray diffraction patterns of the Be-DLA, Mg-DLA, Ca-DLA, Sr-DLA and Ba-DLA adduct products.

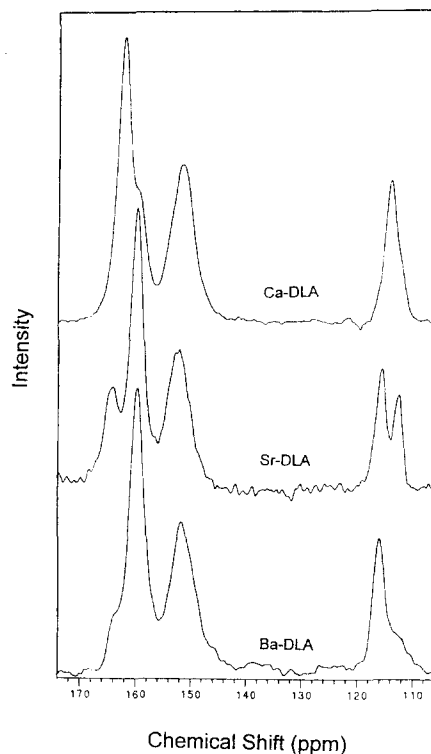


Fig. 8. Solid-state  $^{13}\text{C}$ -NMR spectra obtained for the Ca-DLA, Sr-DLA and Ba-DLA adduct products.

## References

- [1] E.M. Chamot and C.W. Mason, *Handbook of Chemical Microscopy*, Vol. 2, 2nd edn., Wiley, New York, 1940.
- [2] R.E. Dunbar and J. Knuteson, *Microchem. J.*, 1 (1957) 17–37.
- [3] R.E. Dunbar and F. Ferrin, *Microchem. J.*, 4 (1960) 167–179.
- [4] R.E. Dunbar and C.C. Moore, *Microchem. J.*, 3 (1959) 491–505.
- [5] R.E. Dunbar and B.W. Farnum, *Microchem. J.*, 5 (1961) 5–18.
- [6] R.E. Dunbar and A.E. Aaland, *Microchem. J.*, 2 (1958) 113–127.
- [7] R.E. Dunbar and F. Ferrin, *Microchem. J.*, 3 (1959) 65–82.
- [8] R.E. Dunbar and F. Ferrin, *Microchem. J.*, 4 (1960) 59–72.
- [9] R.E. Dunbar and F. Ferrin, *Microchem. J.*, 5 (1961) 145–157.
- [10] E.G.C. Clarke and M. Williams, *J. Pharm. Pharmacol.*, 7 (1955) 255–262.
- [11] E.G.C. Clarke, *J. Pharm. Pharmacol.*, 8 (1956) 202–206.
- [12] E.G.C. Clarke, *J. Pharm. Pharmacol.*, 9 (1957) 187–192.
- [13] E.G.C. Clarke, *J. Pharm. Pharmacol.*, 9 (1957) 752–758.
- [14] E.G.C. Clarke, *J. Pharm. Pharmacol.*, 10 (1958) 194–196.
- [15] E.G.C. Clarke, *J. Pharm. Pharmacol.*, 10 (1958) 642–644.
- [16] E.G.C. Clarke, *J. Pharm. Pharmacol.*, 11 (1959) 629–636.
- [17] C.E. Redemann and C. Niemann, *J. Am. Chem. Soc.*, 62 (1940) 590–593.
- [18] C.V. Francis, *Microchem. J.*, 7 (1963) 375–382.
- [19] B.M. Craven, S. Martinez-Carrera and G.A. Jeffrey, *Acta Cryst.*, 17 (1964) 891–903.
- [20] M.V. Jovanovic and E.R. Clarke, *Heterocycles*, 24 (1986) 3129–3141.